Int. J.Nano Dimens. 3(3): 207-216, Winter 2013
ISSN: 2008-8868

Contents list available at **IJND**

International Journal of Nano Dimension

Journal homepage: *www.IJND.ir*

Influence of current density on refractive index of *p*-type nanocrystalline porous silicon

J. Pandiarajan[1]
N. Jeyakumaran[1]
B. Natarajan[2]
N. Prithivikumaran[1,*]

[1]Nanoscience Research Lab, Department of Physics, V. H. N. S. N. College, Virudhunagar – 626 001, Tamilnadu, India.
[2]Department of Physics, R.D. Government Arts College, Sivagangai – 630 561, Tamilnadu, India.

Received 18 March 2012
Accepted 28 May 2012

* Corresponding author:
N. Prithivikumaran
Nanoscience Research Lab,
Department of Physics,
VHNSN College, Virudhunagar – 626001, Tamilnadu, India.
Tel +91 9486636535
Fax +91 4562 281338
Email janavi_p@yahoo.com

ABSTRACT

Porous Silicon (PS) layers have been prepared from *p*-type silicon wafers of (100) orientation. SEM, XRD, FTIR and PL studies were done to characterize the surface morphological and optical properties of PS. The porosity of the PS samples was determined using the parameters obtained from SEM images by geometric method. The refractive index values of the PS samples as a function of porosity were determined by Effective Medium Approximation methods. The influence of current density on porosity and refractive index of PS, were discussed. SEM images indicated that the pores are surrounded by a thick columnar network of silicon walls. This porous silicon layer can be considered as a sponge like structure. The sizes of PS nanocrystallites were determined by XRD studies. FTIR spectra indicated that the porous layer contain SiHn complexes. PL study reveals that there is a prominent emission peak at 606 nm. No spectral shift was observed. These results suggest that this nanocrystalline porous silicon could be a potential candidate for optical as well as optoelectronic device applications.

Keywords: *Porous silicon; Current density; Porosity; Refractive index; SEM; XRD; FTIR; Photoluminescence; Device applications*.

INTRODUCTION

Silicon has historically been the dominant material for electronics, while work in optoelectronics has relied almost entirely on III – V compound materials such as GaAs and InP. The primary reason for this contradiction is due to the fact that light emission from silicon is impractical because of its indirect band gap structure [1]. The porous silicon (PS) has received increasing attention both from the experimental as well as the theoretical point of view [2-5]. Porous silicon has been studied intensively since the discovery by Canham [1] that even at room temperature PS can emit very bright photoluminescence (PL), in great contrast to crystalline silicon (c-Si).

Porous silicon layers have been prepared by various methods such as electrochemical etching [6], strain etching [7] and laser assisted etching [8] etc., Porous silicon can also be formed by an anodic electrochemical etching technology on single crystal Si surface in hydrofluoric acid (HF) mixed solutions [9,10]. Porous Silicon can exhibit a large variety of morphologies and particle sizes. In all PS applications, information about the pore size, distribution and surface chemistry and their dependence on the fabrication conditions play a decisive role. Principal parameters (HF: ethanol concentration, current density, etching time) controlling PS macro pore formation depend on properties of silicon substrate wafer type, crystal orientation, doping element and resistivity, etching solution and temperature [11]. The main purpose of the present work is to study the influence of current densities on the physical properties of porous silicon, especially refractive index.

EXPERIMENTAL

PS samples were prepared by electro-chemical etching of boron doped p type (1 0 0) oriented Si wafer (ρ = 0 -100 Ω cm) in a 1:1 (48 % HF: 99 % C_2H_5OH) solution for 10 minute at different current densities of 30 mA/cm^2, 40 mA/cm^2, 50 mA/cm^2, 60 mA/cm^2 and 70 mA/cm^2 in a Teflon single tank anodizing system. In this system, the anode was p-Si wafer and the cathode was platinum rod. To characterize the microstructures of porous silicon Hitachi S – 3000 N model Scanning electron microscope with an accelerating voltage of the electron beam of 20 kV was employed. The X-ray Diffraction (XRD) spectra were recorded by using Bruker D8 advanced X-ray diffractometer using CuKα_1 (1.54060 Å) source. The photoluminescence excitation spectra of porous silicon were obtained with a Shimadzu RF 5301 luminescence spectrophotometer. A pulsed xenon lamp was built in the spectrometer as the excitation source. The Fourier Transform Infra Red (FTIR) spectra of the samples were recorded by using the Shimadzu IR affinity - 1 spectrophotometer. All measurements were carried out at room temperature.

RESULTS AND DISCUSSION

SEM analysis

The plane view SEM images of porous silicon prepared with p type silicon substrates of (1 0 0) orientation using 30 mA/cm^2, 40 mA/cm^2, 50 mA/cm^2, 60 mA/cm^2 and 70 mA/cm^2 current densities are shown in Figure 1a - 1f. One of the most important characteristics of a porous silicon layer is its porosity. The porosity of PS is defined as the quantity of silicon removed during anodization compared with the silicon concentration before anodization evaluated in the same volume. The porosity (P) can also be defined as a function of geometrical parameters written as [12, 13],

$$P = \left(\frac{\pi}{2} * 1.732\right)\left(\frac{1}{1+\frac{m}{d}}\right)^2 \qquad (1)$$

Where d is the average pore size and m is the distance between pores. The calculated porosity values from SEM images are tabulated in Table 1.

Figure 1b shows the initiation of silicon etching at 30 mA/cm^2 with larger grains. The etching of the layer has already begun and uniform small pores have been developed in the layer. Using the equation (1), the porosity of 30 mA/cm^2 current density PS, has been estimated as 35 %. At 40 mA/cm^2(Figure 1c), the pores of slightly larger diameter were found to be formed and the pores are surrounded by a thick columnar network of silicon walls. The porosity of this sample is 53%. Further increasing the current density to 50mA/cm^2, the entire surface shows sponge like structure. These observations confirm the presence of nanocrystalline silicon particles around the pores. Figure 1d shows that the pore size distribution is relatively uniform and the columnar silicon walls are very thin and appear to have fairly uniform thickness. The nanocrystalline morphologies were observed all over the surface of the etched Si. A high value of 75 % porosity was obtained in the 50 mA/cm^2 sample. At 60 mA/cm^2, it can be seen from the SEM image (Figure 1e) that some pore walls are broken. The calculated porosity value for this sample is about 40 %. This decrease in porosity value may be due to the reason that the value obtained is the porosity of the second layer of the

surface as a portion of the top layer could have been etched away, exposing the next layer. At the current density of 70 mA/cm^2, the estimated porosity value is 65 % and the Figure 1e & 1f show thicker silicon walls which are observed after the dissolution of the top fine porous layer at higher current densities beyond 50 mA/cm^2 [14, 15].

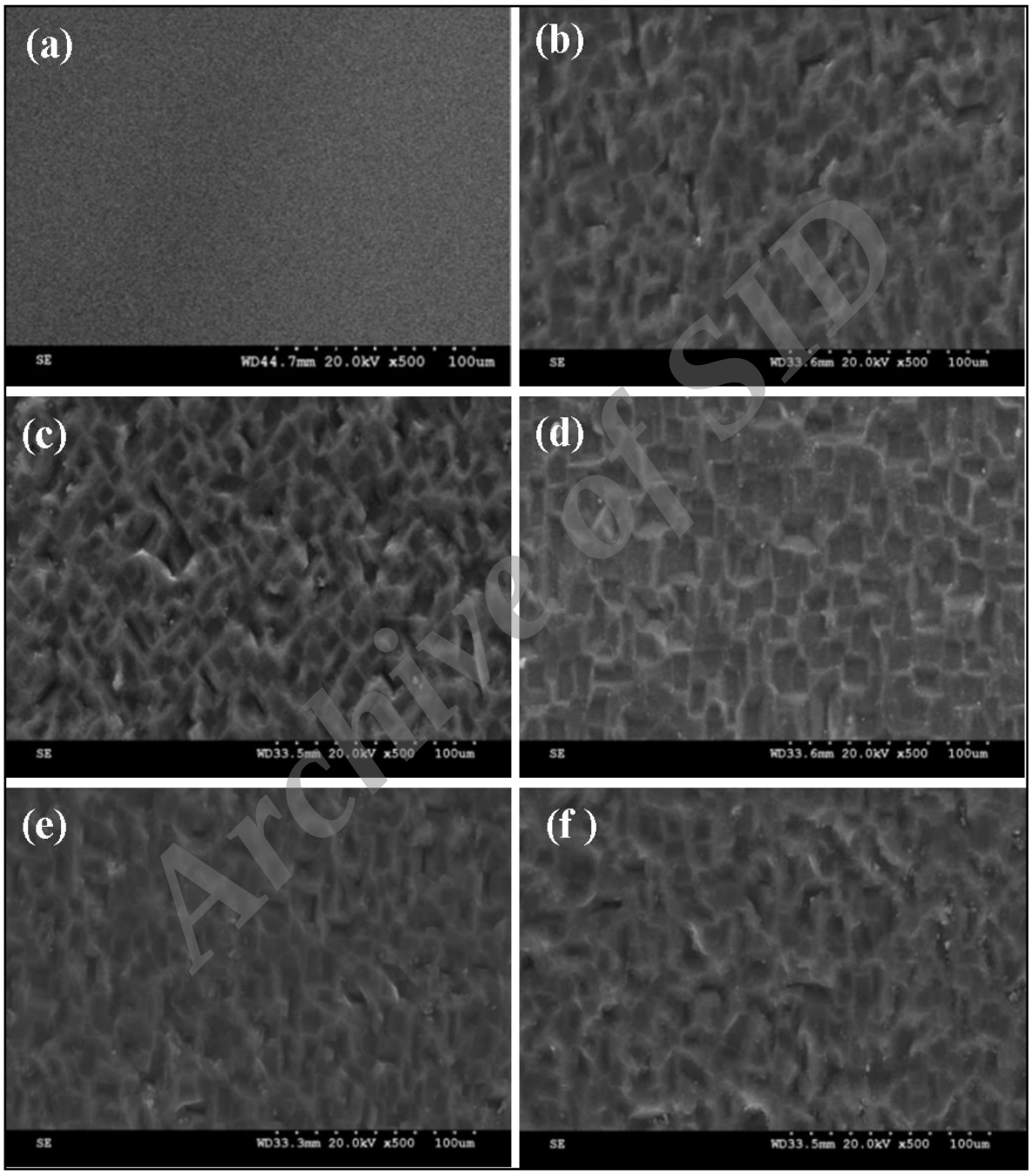

Fig. 1. SEM images of a) single crystal Si and porous silicon structures formed at current densities of b)30 mA/cm^2, c) 40 mA/cm^2, d) 50 mA/cm^2, e) 60 mA/cm^2 and f) 70 mA/cm^2

Table 1. Calculated porosity values of different current densities

Current density	Porosity
30 mA/cm^2	35 %
40 mA/cm^2	53 %
50 mA/cm^2	75 %
60 mA/cm^2	40 %
70 mA/cm^2	65 %

Refractive index determination based on effective medium approximations

The porous silicon is a composite material with a mixture of single crystal silicon (c-Si) and voids. When the void spaces in the host material are much smaller than the wavelength of incident light, the two phase composite material can be considered as a single effective medium. The widely used method to model the optical properties of composite materials is the effective medium approximation (EMA).

In two components system of porous silicon (silicon + air), the refractive index is expected to be lower than the bulk silicon. The Bruggeman [16], Maxwell-Garnett [17] and Looyenga [18] methods are used here to determine the refractive index (n) of porous silicon. These appropriate effective medium models depend on the porosity and morphology of the porous silicon.

The expressions (2), (3) and (4) given by Bruggeman, Looyenga and Maxwell-Garnett describe the refractive index as a function of porosity.

$$n_{PS} = 0.5\left[3P(1-n^2{}_{Si}) + (2n^2{}_{Si}-1) + \left[(3P(1-n^2{}_{Si}) + (2n^2{}_{Si}-1))^2 + 8n^2{}_{Si}\right]^{0.5}\right]^{0.5} \quad (2)$$

$$n^{2/3}{}_{PS} = (1-P)n^{2/3}{}_{Si} + Pn^{2/3}{}_{air} \quad (3)$$

And

$$(1-P)\frac{n^2{}_{Si} - n^2{}_{air}}{n^2{}_{Si} + 2n^2{}_{air}} = \frac{n^2{}_{PS} - n^2{}_{air}}{n^2{}_{PS} + 2n^2{}_{air}} \quad (4)$$

The calculated refractive index values are given in Table 2 along with the literature values. Figure 2 shows a comparison between refractive index values of Bruggeman, Maxwell-Garnett and Looyenga effective medium approximation methods linking the porosity to refractive index.

The plot (Figure 2) between porosity versus refractive index shows that as the porosity increases the refractive index decreases. Of the three effective medium approximation methods the refractive index values obtained from Looyenga method matches well with the literature values. From Table 1 & 2, it could be understood that the porosity is tunable which in turn makes refractive index also tunable and because of the control capability of its refractive index, the application of PS as an antireflection coating is very important.

Figure 3 illustrates the lower refractive index nanocrystalline PS layer which includes air pores, silicon networks over bulk Si in view of optoelectronic and optical device applications.

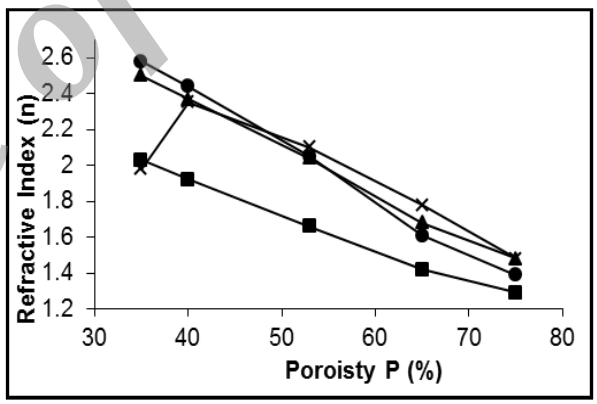

Fig. 2. Comparison of Literature (×) and calculated values of *P* and *n* values using Bruggeman (●), Maxwell-Garnett (■) and Looyenga (▲) Effective Medium approximation methods

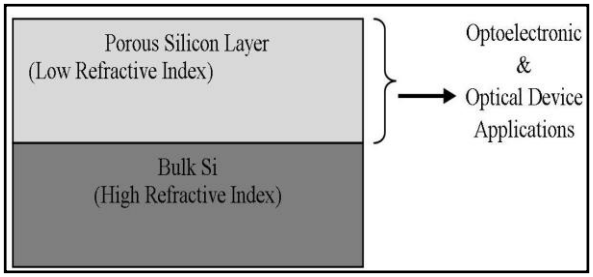

Fig. 3. PS/c-Si layers for device applications

Table 2. Comparison of Calculated and Literature values of *P* and *n* values using Bruggeman, Maxwell-Garnett and Looyenga Effective Medium approximation methods

Porosity *P* (%)	Refractive Index (*n*)			
	Bruggeman Method	Looyenga Method	Maxwell – Garnett Method	Literature Values
35	2.58	2.50	2.03	1.98 (Kordas *et al.*,[19])
40	2.44	2.37	1.92	2.35 (Theiss *et al.*,[20])
53	2.05	2.04	1.66	2.10 (Salem *et al.*,[21])
65	1.61	1.68	1.42	1.78 (Jia *et al.*,[22])
75	1.39	1.48	1.29	1.48 (Jia *et al.*,[22])

XRD analysis

The XRD patterns of porous silicon prepared on *p*-type silicon single crystal wafers with (1 0 0) orientation using different current densities of 30 mA/cm^2,40 mA/cm^2, 50 mA/cm^2, 60 mA/cm^2 and 70 mA/cm^2 are shown in Figure 4(a-c).

The 30 mA/cm^2 sample shows a dominant peak (P1) at 2θ = 69.1260^o along with a peak of lower intensity (P2) at 2θ = 69.0668^o. The peak P1 is due to the crystalline Si substrate corresponding to the reflections from the (4 0 0) set of planes (JCPDS File No.89-2955) [23]. The shorter peak P2 at a lower 2θ position arises from the porous layer and these observations are in accordance with literature reports [24-26].

When the current density was increased to 40 mA/cm^2, there is an enormous fall in the intensity of both the peaks P1 and P2 and the peaks also shift to lower 2θ position.

The grain size (*D*) of the porous silicon was calculated using the Debye-Scherer's formula [27],

$$D=\frac{0.9\lambda}{\beta\cos\theta}(nm) \qquad (5)$$

The grain size value of the porous silicon was found to decrease, from 73 nm for 30 mA/cm^2 sample to 20 nm for 40 mA/cm^2 This fall in gain size is due to increase in the pore size and porosity as shown by SEM study.

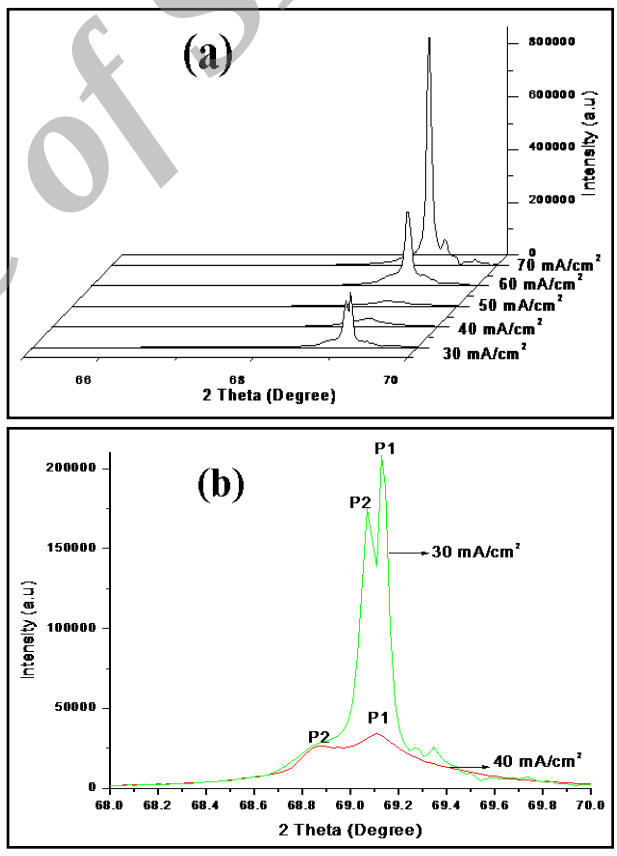

Fig. 4. XRD pattern of porous silicon structures formed at (a) different current densities and (b) P1, P2 peaks view of 30 and 40 mA/cm^2 samples.

At 50 mA/cm^2, the XRD plot shows a single broad peak indicating small and uniform grain sizes of particles all over the etched layer. The grain size was 18 nm for 50 mA/cm^2 sample. Increasing current density further to 60 mA/cm^2, the peak intensity shoots up giving much higher grain size of 128 nm .This may be due to the reason that when the current density was increased above 50 mA/cm^2 the upper layer could have been etched away and the grain size value corresponds to grains of the next layer [28]. The SEM image (Figure 1 e) also shows that some pore walls were broken at this current density. At a higher current density of 70 mA/cm^2 the grain size falls to 102 nm (Table 3).

Photoluminescence analysis

Visual observation of the PS layer showed a greenish yellow reflection for all the current densities. PL spectra were recorded by using an excitation wavelength of 400 nm. Figure 5 shows the room temperature PL spectra obtained for the porous silicon structure formed at 30 mA/cm^2, 40 mA/cm^2, 50 mA/cm^2, 60 mA/cm^2 and 70 mA/cm^2 current densities. The observed PL spectra at room temperature for all the current densities confirm the formation of porous silicon structures with nanocrystalline features.

Table 3. XRD data of porous silicon samples prepared at various current densities

Current Density (mA/cm^2)	2θ (Degree)	Peak Height (a.u)	FWHM	Grain size D (nm)
30	69.0668	175216	0.1380	73
40	69.1062	34252	0.5128	20
50	69.1062	21285	0.5719	18
60	69.1260	279622	0.0789	128
70	69.0865	861611	0.0986	102

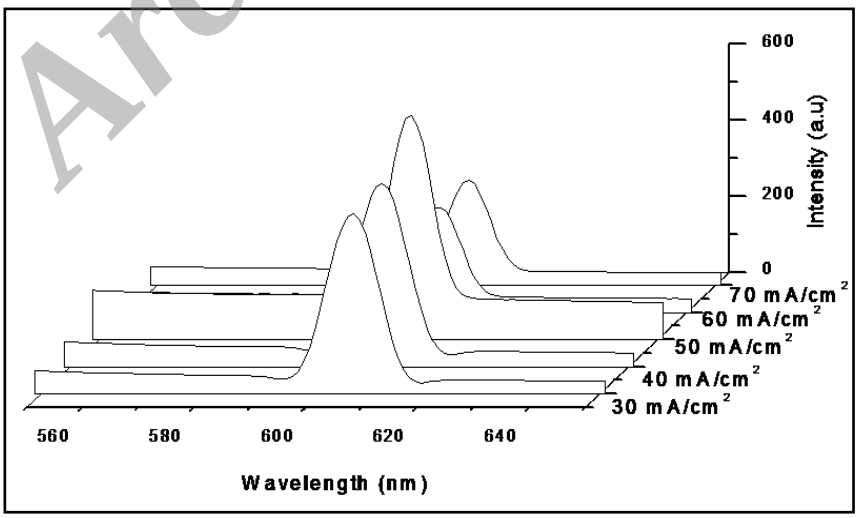

Fig. 5. PL spectra of current density varied porous silicon samples

The Figure 5 shows that there is intense room temperature PL in the visible region for all the current densities employed. Further it can be seen that the maximum PL intensity occurs at 606 nm for all the samples. It is interesting to note that when the current density increases, the PL intensity increases and reaches a maximum for a current density of 50mA/cm^2 and then falls for further increase in current density. At the lower current density of 30mA/cm^2, the SEM image shows the formation of small pores on the surface and in the PL spectrum, this is indicated by relatively low PL intensity. When the current density is increased to 40 mA/cm^2, uniform pores with increased diameter were obtained and this is reflected by a rise in the PL intensity. SEM study shows that at 50 mA/cm^2 current density the porosity is maximize and this is supported by maximum PL intensity. This indicates that 50 mA/cm^2 current density is the best suited for the *p*-type silicon to prepare PS in order to obtain maximum PL emission. It is highly likely that the increase of the PL intensity is caused by increase in the total volume of the nanocrystallites on the surface of the PS [29]. When the current density is further increased to 60 mA/cm^2, the peak intensity of PL is decreased. It is caused by the decrease in the volume of fraction of the nanocrystallites and due to the breaking of pore walls exposing the next layer. However there is no apparent shift in the PL peak position in spite of the pore widening (Table 4). The samples exhibit a PL band in the red region.

Table 1. Calculated porosity values of different current densities

Current density	Porosity
30 mA/cm^2	35 %
40 mA/cm^2	53 %
50 mA/cm^2	75 %
60 mA/cm^2	40 %
70 mA/cm^2	65 %

FTIR studies

The FTIR spectra of the porous silicon samples with different current densities of 30 mA/cm^2, 40 mA/cm^2, 50 mA/cm^2, 60 mA/cm^2 and 70 mA/cm^2 are presented in Figure 6.

The spectral peaks give information about the changes in chemical composition of the PS structure. It is necessary to know the chemical composition of PS because the optical and electrical properties depend on impurity content and surface passivation. The original impurity which is always found in PS layers is hydrogen. Infrared absorption experiments have shown the presence of Si ± H_x groups (x = 1, 2, 3….n) on the internal PS surface during the etching process [30, 31].

In Figure 6, strong peaks are observed in the 2000 to 2200 cm^{-1} region which is assigned to Si-H_x bonds [32]. The strong peaks observed at 2250 and 2190 cm^{-1} are due to the O_3SiH stretching mode and SiH-SiO_2 structural group respectively. The strong absorbance bands observed at 2140, 2106 and 2087 cm^{-1} are associated with silicon hydride and dihydride bonds. The presence of hydrogen complexes SiH, SiH_2, SiH_3……SiH_n was suggested to explain the luminescence of PS [13, 33]. These Si-H_n bonds provide a very good passivation of the defects and allow very attractive radiative efficiencies to be obtained [32]. From the Figure 6, it can be seen that the porous silicon structures formed in the present study are mainly hydrogen passivated. Such results have been reported by Zhang *et al.*[34] and Kim *et al.*[29] They have established that hydrogenation not only eliminates the dangling bond states from the energy gap, but also widens the energy gap.

The FTIR absorption peak intensity of SiH_n complexes increases with current density and is maximum for 50mA/cm^2 and then the intensity falls for further increase of current density. Thus the chemisorptions of SiH_n in the PS layer appear to be closely linked to the variation in PL intensity. The results of the present study also indicate that SiH_n plays a key role to the observed luminescence process.

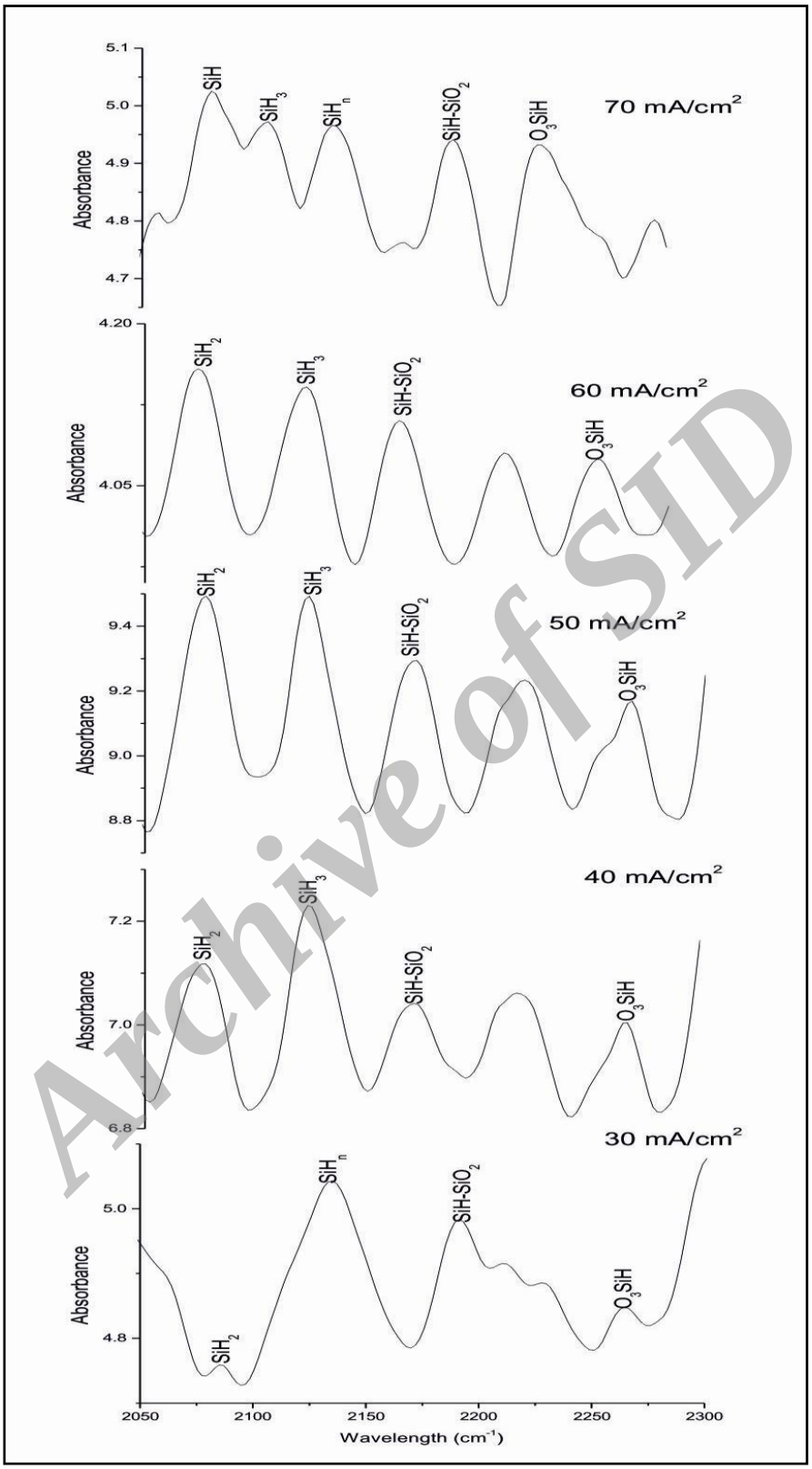

Fig. 6. FTIR spectra of PS samples prepared using different current densities

CONCLUSIONS

The porosities of the current density varied PS samples were determined from SEM images by geometrical method. The corresponding refractive indices were obtained through effective medium approximation methods and of the three EMA methods the Looyenga method fit well for the PS samples of different porosities. Since the Looyenga method is applicable for densely packed composites and it considers an interconnected network for all porosities the results for refractive index obtained by this method are better than other methods particularly for PS. SEM analysis also show a uniform distribution of pores in the porous layers. Visible PL was observed at 606 nm for all the PS samples prepared with different current densities. The sample exhibits a PL band at red region and intensity increases with respect to current density, suggesting that hydride related luminescence process may be active in PS. The occurrence of strong PL & FTIR spectra may be attributed to the transition among the quantum confined states in nanoscale Si, which are influenced by the surface bonds. The XRD and PL studies confirm the presence of silicon nanocrystallites and networks in the PS structure. The observed variation in refractive index and PL emission intensity with respect to current density shows that porous silicon can be a promising candidate to be used as antireflection layer in solar cells and in intensity varying light emitting diode applications.

ACKNOWLEDGEMENTS

The authors are grateful to the University Grants Commission, New Delhi for extending financial support to carry out this work under Major Research Project [F.No.35-20/2008 (SR)].

REFERENCES

[1] Canham, L.T., (1990). Silicon quantum wire array fabrication by electrochemical and chemical dissolution of wafers, *Appl. Phys. Lett.* 57, 1046-1048.

[2] Vial, J.C., Bsiesy, A., Gaspard, F., Herino, R, Ligcon, M., Mullar, F., Romestein, R., and Macfalne, R.M.,(1992). Mechanisms of visible-light emission from electro-oxidized porous silicon, *Phy. Rev. B.* 45, 14171-14176.

[3] Lehmann, V., and Gosele, U., (1991). Porous silicon formation: A quantum wire effect, *Appl. Phys.Lett.*58, 856 – 858.

[4] Brandt, M. S., Fuches, H.D., Stutzmann, M., Weber, J., and Cardona, M., (1992). The origin of visible luminescencefrom "porous silicon": A new interpretation, *Solid State Comm.*81, 307 - 312.

[5] Sandres, G. D., and Chang, Y. C., (1992). Theory of optical properties of quantum wires in porous silicon, *Phys.Rev.B.*45, 9202 - 9213.

[6] Natarajan, B., Ramakrishan, V., Vasu, V., and Ramamurthy, S., (2006). Structural and Photoluminescence Properties of Porous Silicon: Effect of HF Concentration, *Surface Review and Letters* 13(4), 351-356.

[7] Yoshioka, S., Takayangi, S., (1965). Stain Films on Silicon, *Jpn. J. Appl. Phys.*4, 828-830.

[8] Rajeshkumar, Mavi, H.S., Shukla, A.K., (2008). Macro and microsurface morphology reconstructions during laser-induced etching of silicon, *Micron* 39, 287-293.

[9] Smith, R.L., and Collins, S, D., (1992). Porous silicon formation mechanisms, *J. Appl. Phys.*71, R1.

[10] Halimouiin, A; Vial, J.C., and Derrien, J., (1994) *Porous Silicon and Technology*, Lesullis, p.33

[11] Dian, J., Macek, A., Nizansky, D., Nemec, I., (2004) SEM and HRTEM study of porous silicon—relationship between fabrication, morphology and optical properties, *Appl. Surf. Sci.* 238, 169-174.

[12] Salcedo, W.J., Fernandez, F. J. R., and Galeazzo, E., (1997). Structural Characterization of Photo luminescent Porous Silicon with FTIR Spectroscopy, *Brazilian J. Phys.*27 158-161.

[13] Natarajan, B., Ramakrishan, V., Vau, V., and Ramamurthy, S., (2005). Structural and Photoluminescence Properties of Porous Silicon: Effect of Surface Passivation, *Surface Review and Letters*, 12 (4), 645-649.

[14] Gosele, U., Lehmann, V., Feng, Z.C., Tsu, R., (1994). *Porous Silicon* (Singapore; World Scientific) p.17
[15] Campbell, S.D., Jones, L. A., Nakamichi, E., Wei, F.X., Zajchowski, L.D., Thomas, D.F., (1995). *J. Vac. Sci. Tech. B.*15, 1184.
[16] Bruggeman, D.A.G., (1935). Berechnung verschiedener physikalischer Konstanten von heterogenen Substanzen, *Ann. Phys. (Leipzig)* 24, 636-679.
[17] Garnett,J.C.M., (1904). Colours in metal glasses and in metallic films, *Phil.Trans.R.Soc.Lond.*203,385–420.
[18] Looyenga, H., (1965). Dielectric constants of heterogeneous mixtures, *Physica* 31, 401-406.
[19] Kordas, K., Pap, AE., Beke, S., Leppavuori, S., (2004). Optical properties of porous silicon: Part I: Fabrication and investigation of single layers, *Optical Materials* 25, 251-255.
[20] Theiss, W., Hilbrich, S., (1997). Refractive index of porous silicon in *Properties of Porous Silicon* 223-228.
[21] Salem, M.S., Sailor, M. J., Sakka, T., and Ogata, Y.H., (2007). Electrochemical preparation of a rugate filter in silicon and its deviation from the ideal structure, *J. Appl. Phy.* 101, 063503-063508.
[22] Jia, (2005). Determination of the effective refractive index of porous silicon/polymer composite films, *Chinese Optics Letters*, 3 (10), 608-610.
[23] JCPDS File No. 89-2955 (International Centre for Diffrcation Data) Newton Square, PA, U.S.A.
[24] Tischler, (1996). *Phys. Today* 50, 24.
[25] Chambard, V., Setzu, S., and Romestain, R., (2002). Light assisted formation of porous silicon investigated by X-ray diffraction and reflectivity, *Appl. Surf.Sci.*191, 319-327.
[26] Buttard, D., Bellet, D., and Baumbach, T., (1996). X-ray diffraction investigation of porous silicon superlattices, *Thin Solid Films* 276, 69-72.
[27] Culity, B.D., *Elements of X-ray Diffraction* (Addition-Wesley Pub.Co.) 1956.
[28] Vidhya, V.S., Padmavathy, P., Murali, K.R., Sanjeeviraja, C., Manishankar, P., Jayachandran, M., (2011). Development of porous silicon matrix and characteristics of porous silicon/tin oxide structures, *Journal of Non-Crystalline Solids* 357, 1522-1526.
[29] Kim, D.A., Shim, J.H, Cho, N.H., (2004). PL and EL features of *p*-type porous silicon prepared by electrochemical anodic etching, *Appl. Surf. Sci*. 234, 256-261.
[30] Prokes, S. M., Freitas, J. A., Searson, P. C., (1992). Microluminescence depth profiles and annealing effects in porous silicon, *Appl. Phy. Lett.*60 (26), 3295-3297.
[31] Borghesi, A., Sassella, A., Pivac, B., Pavesi, L., (1993). Characterization of porous silicon inhomogeneities by high spatial resolution infrared spectroscopy, *Solid State Commun*. 87, 1-4.
[32] Borghesi, A., Guizzetti, G., Sassella, A., Bisi, O., Pavesi, L., (1994). Induction-model analysis of Si-H stretching mode in porous silicon, *Solid State Commun*. 89, 615-618.
[33] Hory, M.A., Herino, R., Lingeon, M., Muller, F., Gaspard, F., Mihalcescu, I., Vial, J. C., (1995). Fourier transform IR monitoring of porous silicon passivation during post-treatments such as anodic oxidation and contact with organic solvents, *Thin Solid Films* 225, 200-203.
[34] Zang,X.G.,(1991).Mechanism of Pore Formation on n-Type Silicon, *J. Electro. Chem. Soc.*138, 3750-3756.

Cite this article as: J. Pandiarajan *et al.*: Influence of current density on refractive index of *p*-type nanocrystalline porous silicon.
Int. J.Nano Dimens. 3(3): 207-216, Winter 2013